Model of ion transport regulation in chloride-secreting airway epithelial cells

Integrated description of electrical, chemical, and fluorescence measurements

Thomas Hartmann and A. S. Verkman

Departments of Medicine and Physiology, the Cystic Fibrosis Research Center, and the Cardiovascular Research Institute, University of California, San Francisco, California 94143 USA

ABSTRACT An electrokinetic model was developed to calculate the time course of electrical parameters, ion fluxes, and intracellular ion activities for experiments performed in airway epithelial cells. Model variables included cell [Na], [K], [Cl], volume, and membrane potentials. The model contained apical membrane Cl, Na, and K conductances, basolateral membrane K conductance, Na/K/2 Cl and Na/Cl symport, and 3 Na/2 K ATPase, and a paracellular conductance. Transporter permeabilities and ion saturabilities were determined from reported ion flux data and membrane potentials in intact canine trachea. Without additional assumptions, the model predicted accurately the measured short-circuit current (I_{sc}), cellular conductances, voltage-divider ratios, open-circuit potentials, and the time course of cell ion composition in ion substitution experiments. The model was used to examine quantitatively: (*a*) the effect of transport inhibitors on I_{sc} and membrane potentials, (*b*) the dual role of apical Cl and basolateral K conductance in cell secretion, (*c*) whether the basolateral symporter requires K, and (*d*) the regulation of apical Cl conductance by cAMP and Ca-dependent signaling pathways. Model predictions gave improved understanding of the interrelations among transporting systems and in many cases gave surprising predictions that were not obvious without a detailed model. The model developed here has direct application to secretory or absorptive epithelial cells in the kidney thick ascending limb, cornea, sweat duct, and intestine in normal and pathophysiological states such as cystic fibrosis and cholera.

INTRODUCTION

There are a number of physiologically similar Cl-secreting epithelia which contain a regulated Cl conductance contralateral to cation/Cl symport and K conductance. In tracheal epithelial cells (Fig. 1), Na/K/2 Cl, or Na/Cl symport is driven by electrochemical gradients established by the 3 Na/2 K ATPase; Cl is driven through apical Cl channels. Other epithelia which function in a similar manner include the intestine, sweat duct, cornea, and kidney thick ascending limb. In the disease states cystic fibrosis and cholera, one or more ion channels are selectively malregulated, resulting in marked hyposecretion or hypersecretion of Cl.

We focus here on the development of an accurate kinetic model of canine airway epithelial cells. This cell system has been used extensively in studies of airway secretory function in normal and disease states. There are a number of overlapping and complementary parameters that have been measured in these cells including short-circuit current (I_{sc}), tracer ion fluxes, open-circuit and short-circuit membrane potentials, and intracellular ion concentrations using microelectrodes and fluorescent indicators. Both steady-state and non-steady-state measurements have been performed in response to selected agonists, inhibitors, or ion substitution. Despite a significant body of published experimental data, a number of basic issues remain unresolved such as the cation requirement of the basolateral symport mechanism and the sites(s) of action of Ca and cAMP agonists.

In analyzing the complex effects of Ca and cAMP agonists on I_{sc}, transepithelial conductances, and intracellular Ca (Hartmann et al., 1989), it became clear that a mathematical model was necessary to interpret the data and to design experiments to distinguish among competing hypotheses. We have therefore developed a quantitative electrokinetic model of canine tracheal epithelial cells based on the general mathematical formulation developed by Latta et al. (1984) and extended by Verkman and Alpern (1987). When formulated with a minimal set of assumptions, the model accurately reproduced a number of important published observations. The model was used to understand conceptually the complex interactions among transporting systems when the tracheal epithelium is exposed to selected transporter inhibitors and agonists. Unresolved issues in the mechanism of transport regulation in the airway were examined and new experimental strategies were suggested.

We believe that the model will be helpful in the analysis of experimental data for several cell types when a suitable selection of parameters is made. The source code of the

Address correspondence to Dr. A. S. Verkman, 1065 HSE, Box 0532, University of California, San Francisco, CA 94143.

0006-3495/90/08/391/11 $2.00

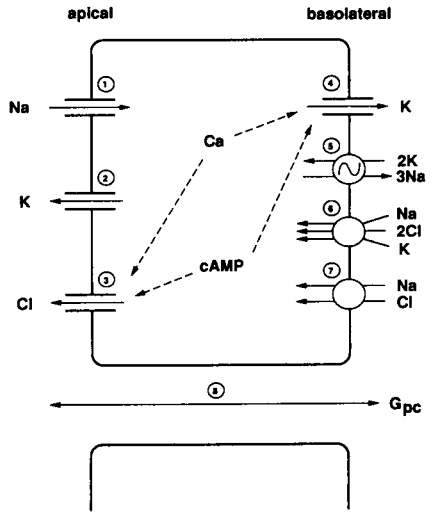

FIGURE 1 Ion transport mechanisms in canine tracheal epithelium. Individual transporters are numbered according to the indices used in Eqs. 1–5. Transporter stoichiometries are given. Two of the proposed Ca and cAMP-dependent sites of action are indicated by dashed lines.

model presented is available from the authors upon request.

MODEL FORMULATION

Overview

A monolayer of homogeneous cells containing transcellular and paracellular transporting pathways was modeled under short-circuit and open-circuit conditions. Model parameters included intracellular activities of Na, K, and Cl, cell membrane potentials, and cell volume. It was assumed that the composition of solutions bathing the mucosal and serosal surfaces could be specified and changed at any time without unstirred layer effects.

The transporting systems included in the model are given in Fig. 1. Transporter permeability coefficients were determined from steady-state ion flux data and membrane potentials. Transporter saturabilities and allosteric dependences were included if known; if not known, the transporters were assumed to function according to thermodynamic equations. The basic kinetic formulation of the model and its iterative solution for open-circuit and short-circuit boundary conditions was developed and reported for studies of the regulation of acidification in the kidney proximal tubule (Verkman and Alpern, 1987).

Flux equations

The relationship between transporter fluxes and the electrochemical driving force must be specified for each transport system. For the four single ion conductances in the model, apical Cl, Na, and K conductances, and basolateral K conductance, the transport equations are:

$$J_1 = P_1 \cdot U_a \cdot ([Na]_a - [Na]_c \cdot e^{-Ua})/(1 - e^{-Ua}) \quad (1a)$$

$$J_2 = P_2 \cdot U_a \cdot ([K]_a - [K]_c \cdot e^{-Ua})/(1 - e^{-Ua}) \quad (1b)$$

$$J_3 = P_3 \cdot U_a \cdot ([Cl]_a \cdot e^{-Ua} - [Cl]_c)/(1 - e^{-Ua}) \quad (1c)$$

$$J_4 = P_4 \cdot U_b \cdot ([K]_b - [K]_c \cdot e^{-Ub})/(1 - e^{-Ub}). \quad (1d)$$

J_i is the turnover rate of transporter i (transporter identification given in Fig. 1) in units of $\mu eq \cdot cm^{-2} \cdot h^{-1}$, and $[X]_a$, $[X]_b$, and $[X]_c$ are the apical, basolateral, and cell activities of ion X, respectively. J_i was defined as positive in Eqs. 1*a–d* when i moves into the cell. U_a and U_b are dimensionless apical and basolateral membrane potentials ($U = \psi F/RT$, where ψ is membrane potential in millivolts and RT/F ~27 mV at 37°C), and P_i is the permeability coefficient for transporter i.

The turnover rate of the 3 Na/2 K ATPase (basolateral transporter 5) was expressed in a manner similar to that of Latta et al. (1984) with saturation constants of $K_{Na} = 11.8$ mM for intracellular Na and $K_K = 1.4$ mM for serosal K (Westenfelder et al., 1980). In addition, a weak dependence of the 3 Na/2 K ATPase turnover rate on basolateral membrane potential has been included according to the recent data of Goldschlegger et al. (1987) in reconstituted vesicles and others (Lederer and Nelson, 1984; Milanick and Hoffmann, 1986; Rakowski et al., 1989; see Apell, 1989, for review) using specific cell types,

$$J_5 = P_5\left[\frac{[Na]_c}{[Na]_c + K_{Na}}\right]^3\left[\frac{[K]_b}{[K]_b + K_K}\right]^2(a \cdot U_b + b), \quad (2)$$

where $a = 0.006\ mV^{-1}$ and b is calculated so that $(a \cdot U_b + b) = 1$ when U_b is the steady-state reduced membrane potential. One turnover of the 3 Na/2 K ATPase is defined as movement of 2 K into and 3 Na out of the cell.

The turnover rates of the electroneutral Na/K/2 Cl and Na/Cl symporters (basolateral transporters 6 and 7) were expressed as hybrid thermodynamic/kinetic equations as discussed by Verkman and Alpern (1987),

$$J_6 = P_6\frac{[Na]_b[K]_b[Cl]_b^2 - [Na]_c[K]_c[Cl]_c^2}{\left[\frac{[Na]_c}{K_{Na}} + 1\right]\left[\frac{[K]_c}{K_K} + 1\right]\left[\frac{[Cl]_c}{K_{Cl}} + 1\right]^2} \quad (3)$$

$$J_7 = P_7\frac{[Na]_b[Cl]_b - [Na]_c[Cl]_c}{\left[\frac{[Na]_c}{K_{Na}} + 1\right]\left[\frac{[Cl]_c}{K_{Cl}} + 1\right]}. \quad (4)$$

Saturability values of $K_{Na} = 3.8$ mM, $K_K = 7.5$ mM, and $K_{Cl} = 26$ mM were estimated from data on epithelial and

nonepithelial cells (McRoberts et al., 1982; Owen and Prastein, 1985; O'Grady et al., 1986). In subsequent modeling, the K dependence of the symporter was examined by setting P_6 or P_7 to zero. One turnover of the Na/K/2 Cl symporter moves 1 Na, 1 K, and 2 Cl into the cell; one turnover of the Na/Cl symporter moves 1 Na and 1 Cl into the cell. Unless otherwise specified, Cl transport across the basolateral membrane was assumed to be mediated by Na/K/2 Cl symport.

A simple paracellular conductance was included in the model for open-circuit calculations. Because external ion activities were fixed in the calculations, a "generic" paracellular conductance was defined as,

$$J_8 = P_8(U_b - U_a), \tag{5}$$

where positive J_8 moves positive charges from mucosal to serosal solutions.

Numerical solution

Given any set of P_i and ion activities at time t, the model calculates a new set of cell Na, K, and Cl activities, volume and membrane potentials at time $t + Dt$. Cell membrane potentials (U_1 and U_2) were determined iteratively by the nonlinear Newton's method from requirements of electroneutrality. Total ionic currents (units of $\mu mol \cdot cm^{-2} \cdot h^{-1}$) across the apical membrane (I_a), basolateral membrane (I_b), and paracellular space (I_{pc}) were,

$$I_a = J_1 + J_2 - J_3 \tag{6a}$$

$$I_b = J_5 - J_4 \tag{6b}$$

$$I_{pc} = J_8, \tag{6c}$$

where the positive current was defined as positive charge movement in the mucosal-to-serosal direction. For short-circuit boundary conditions, $I_a = I_b$ and $U_a = U_b$. For open-circuit conditions $I_a = I_b = -I_{pc}$.

To calculate $[Na(t + Dt)]_c$, $[K(t + Dt)]_c$, and $[Cl(t + Dt)]_c$, the new cell volume, $V(t + Dt)$ was first calculated assuming instantaneous osmotic equilibration, a valid assumption based on the rapidity of water movement compared with ion movement,

$$V(t + Dt) = V(t) \cdot 290/\{121 + [Na(t + Dt)]_c + [K(t + Dt)]_c + [Cl(t + Dt)]_c\}. \tag{7}$$

To establish initial osmotic equilibrium it was necessary to include 121 mosmol/1 H_2O of impermeable intracellular solute. There was very little influence of water movement on model predictions because cell volume generally changed by <10%. However, in simulations of ion substitution or inhibition of the 3 Na/2 K ATPase, volume changes up to 35% were predicted. The new intracellular ion activities were calculated from the equations,

$$[Na(t + Dt)]_c = ([Na(t)]_c V(t) + a_{Na}(J_1 - 3J_5 - J_6)Dt)/V(t + Dt) \tag{8a}$$

$$[K(t + Dt)]_c = ([K(t)]_c V(t) + a_K(J_2 + J_4 + 2J_5 + J_6)Dt)/V(t + Dt) \tag{8b}$$

$$[Cl(t + Dt)]_c = ([Cl(t)]_c V(t) + a_{Cl}(J_3 + 2J_6)Dt)/V(t + Dt), \tag{8c}$$

where activity coefficients a_{Na}, a_K, and a_{Cl} were taken to be 0.75. The full time course of $[Na]_c$, $[K]_c$, $[Cl]_c$, V, U_a, and U_b was calculated by repetition of the above procedure. P_i values or external ion activities could be changed at any time to simulate experimental conditions. In short-circuit calculations, the short-circuit current (I_{sc}) is I_a; transcellular conductance, G, was calculated by Ohm's Law,

$$G = \Delta I_{sc}/\Delta(U_a + U_b), \tag{9}$$

where ΔI_{sc} is the difference in I_{sc} due to a $\Delta(U_a + U_b) =$ 0.1 mV transepithelial potential applied under short-circuit boundary conditions.

Modeling of transport regulation

Ca and cAMP-dependent effects on apical Cl conductance and basolateral K conductance were modeled. Because of the paucity of quantitative data regarding signaling mechanisms, it was necessary to make a minimal set of assumption. Based on measurements of Ca kinetics in primary cultures of dog airway epithelium using fura-2 (Hartmann et al., 1989) the cell Ca transient (in nanomolar) in response to Ca agonists was described by the relation,

$$[Ca]_c(t) = 100 + 450\,[\exp(-0.035t) - \exp(-0.25t)], \tag{10}$$

where t is time after agonist addition in seconds. A linear coupling relationship between permeability coefficient and $[Ca]_c$ was assumed,

$$P_*(t) = P_*(0)(A \cdot [Ca]_c(t) - B), \tag{11}$$

where $P_*(t)$ is P_2 or P_4 at time t, and A and B are coupling constants which give the magnitude of conductance activation. The effect of activation of the cAMP-dependent pathway was described by the empirical relation,

$$P_*(t) = P_*(0)C \cdot [1 - 0.9 \cdot \exp(-0.002t)], \tag{12}$$

where C is a coupling constant (see Results). Stimulation

by both Ca and cAMP-dependent pathways was assumed to be additive.

Computer calculations

The model was implemented in BASIC on an AT-compatible computer. Generally 600 time intervals were chosen for a 60-s simulation which required ~30 s of computing time. The iterative procedures were convergent in all simulations tested.

Parameter selection

Table 1 gives the cell and solution activities of Na, K, and Cl, net ion fluxes and membrane potential for dog tracheal epithelium in its secretory state. Cell activities were taken from intracellular microelectrode studies (Shorofsky et al., 1984; Smith and Frizzell, 1984; Shorofsky et al., 1986). Solution activities were those of a typical extracellular buffer used in experimental protocols which were modeled mathematically. Cell height was estimated to be 50 μm in intact trachea and 5 μm in primary cultures of airway epithelium based on micrographic data of Widdicombe et al. (1981, 1987). Cell membrane potential under steady-state short-circuit conditions was -46 mV based on measurements of Welsh (1983*c*, 1987). Transporter permeability coefficients were calculated from control ion activities, potentials, and measured transcellular net ion fluxes of -1.91 μmol $\cdot$ cm^{-2} $\cdot$ h^{-1} for Cl and 0.74 μmol $\cdot$ cm^{-2} $\cdot$ h^{-1} for Na (see Finkbeiner and Widdicombe, 1990, for review). P_i values used to model primary cultures of dog trachea were calculated from net ion fluxes and membrane potentials given in the legends to Figs. 4 and 5.

TABLE 1 Cell parameters of dog tracheal epithelium

Ion activities	External solution	Cell
	mM	
[Na]	105	21
[K]	4	69
[Cl]	93	37
Net ion fluxes	J^{tc}_{Na}	0.74 $\mu eq \cdot cm^{-2} \cdot h^{-1}$
	J^{tc}_{Cl}	-1.91 $\mu eq \cdot cm^{-2} \cdot h^{-1}$
Membrane potential	V_a	-46 *mV*

References for parameter selection are given in the text. J^{tc}_{Na} and J^{tc}_{Cl} are steady-state transcellular ion fluxes defined as positive for ion movement from mucosal to serosal solutions. Apical membrane potential is given for short-circuited conditions. [Cl] and [K] were measured under short-circuited conditions, whereas [Na] was estimated from an open-circuit measurement.

RESULTS

Steady-state characteristics of the model

The transporter permeability coefficients that were selected as described above are listed in Table 2. Using these parameters, the cell concentrations, volume, and membrane potential remain stable over time at $[Na]_c$ = 21 mM, $[K]_c$ = 93 mM, $[Cl]_c$ = 37 mM, V = 5 μl $\cdot$ cm^{-2}, and U_a = -46 mV for epinephrine stimulated cells under short-circuit conditions. The transporter turnover rates under short-circuit control conditions are given in Table 2. The ion currents and the fluxes of individual ions across the apical and basolateral membranes are equal in the steady-state, as required.

There are several predictions of the model in steady-state conditions that can be compared with reported values. The fractional resistance, defined as apical resistance divided by the sum of apical and basolateral resistance was 0.50 under short-circuit conditions, similar to values of 0.59 and 0.46 measured by intracellular potential-sensitive microelectrodes (Welsh, 1983*d*; Smith et al., 1984). I_{sc} was 2.61 μeq $\cdot$ cm^{-2} $\cdot$ h^{-1}, similar to experimental values reported ranging from 2.3 to 3.0 μeq $\cdot$ cm^{-2} $\cdot$ h^{-1} (see Finkbeiner and Widdicombe, 1990, for review). Under open-circuit conditions, apical and basolateral membrane potentials U_a and U_b were -34 and -57 mV with a paracellular conductance G_{pc} of 2.1 mS $\cdot$ cm^{-2}, giving a transepithelial potential of 23 mV, similar

TABLE 2 Permeability coefficients and steady-state fluxes

	P_i	units	J_i $\mu eq \cdot cm^{-2} \cdot h^{-1}$
Apical membrane			
1 Na conductance	$3.44 \cdot 10^{-3}$	$cm \cdot h^{-1}$	0.74
2 K conductance	$2.54 \cdot 10^{-3}$	$cm \cdot h^{-1}$	-0.04
3 Cl conductance	$4.23 \cdot 10^{-2}$	$cm \cdot h^{-1}$	-1.91
Basolateral membrane			
4 K conductance	$1.24 \cdot 10^{-1}$	$cm \cdot h^{-1}$	-2.04
5 3 Na/2 K ATPase	3.93	$\mu mol \cdot cm^{-2} \cdot h^{-1}$	0.57
6 Na/K/2 Cl symporter	$5.26 \cdot 10^{-4}$	$cm \cdot h^{-1} \cdot M^{-3}$	0.96
7* Na/Cl symporter	$1.30 \cdot 10^{-3}$	$cm \cdot h^{-1} \cdot mM^{-1}$	1.91

P_i were calculated from activities, membrane potential, and steady-state transcellular fluxes given in Table 1 as described in the text.

*In most simulations the basolateral symporter was assumed to be K dependent (P_7 = 0). In simulations in which the symporter was K independent (P_6 = 0), J_i (in units of μeq $\cdot$ cm^{-2} $\cdot$ h^{-1}) were: J_2 = -0.04, J_4 = -1.73, and J_5 = 0.88. Corresponding P_i were: P_2 = 2.14 $\cdot$ 10^{-3} cm $\cdot$ h^{-1}, P_4 = 0.105 cm $\cdot$ h^{-1}, and P_5 = 6.15 μmol $\cdot$ cm^{-2} $\cdot$ h^{-1}. Permeability coefficients and steady-state fluxes of transporter 1, 3, and 7 were as given in Table 2.

to reported values (Smith and Frizzell, 1984; Shorofsky et al., 1986). Under these conditions the transepithelial conductance was 3.3 mS · cm^{-2}, similar to that reported by Welsh (1983*c*). Therefore, steady-state predictions of the model under open- and short-circuit conditions are in good agreement with experimental results.

Non-steady-state response to transport inhibitors

Fig. 2 shows the time course of I_{sc} and membrane potential under short circuit conditions in response to addition of a series of inhibitors commonly used to examine transport mechanisms. The inhibitors and transporters are: ouabain – 3 Na/2 K ATPase, furosemide – Na/K/2 Cl symporter, amiloride – Na conductance, barium – K conductance, and diphenylamine-2-carboxylate (DPC) – Cl conductance. The height of the spikes on I_{sc} curves represent transcellular tissue conductance in units of milliSiemens per square centimeter as given in the scale bar.

Inhibition of the 3 Na/2 K ATPase (Fig. 2 *A*) resulted in a decrease in I_{sc} with a half-time of ~12 min, similar to that of 8 and 12 min reported by Widdicombe et al. (1979) and Welsh (1983*a*). There was a small rapid depolarization due to inhibition of pump current, followed by a slower depolarization due to ionic equilibration.

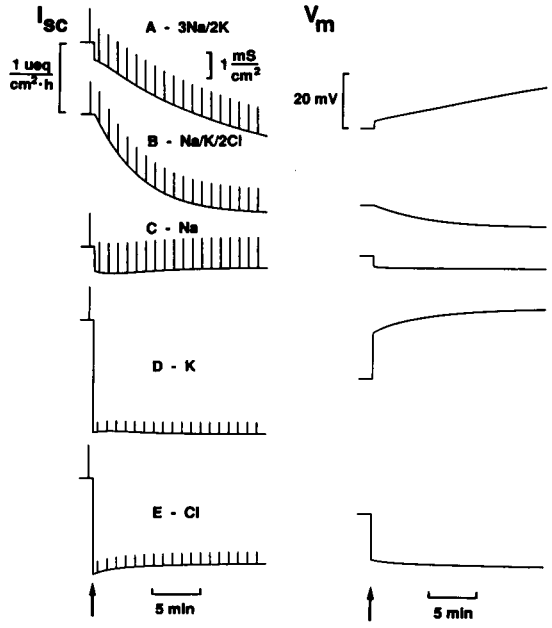

FIGURE 2 Effects of inhibition of individual ion transport mechanisms on short-circuit current (*left*) and membrane potential (*right*). The current spikes represent transcellular conductance (see scale bar for units). In all simulations P_i has been decreased to 10% of its initial value (at arrow) given in Table 1. Initial I_{sc} was 2.61 μeq · cm^{-2} · h^{-1} and V_m was −46 mV. Inhibition of the 3 Na/2 K ATPase (*A*), Na/K/2 Cl symporter (*B*), apical Na conductance (*C*), basolateral K conductance (*D*), and Cl conductance (*E*) are shown.

90% inhibition of the Na/K/2 Cl symporter (Fig. 2 *B*) resulted in a time-dependent decrease in I_{sc} to ~50% of its initial value with a half-time of 5 min which was due to a decrease in Cl secretion from 1.91 to 0.40 μeq · cm^{-2} · h^{-1}. $[Cl]_c$ fell from 37 to 10 mM because of membrane hyperpolarization and inhibition of Cl entry via the symporter. Na absorption (J^{tc}_{Na}, transcellular Na flux) was enhanced slightly (0.74 to 1.02 μeq · cm^{-2} · h^{-1}) after inhibition of the cotransporter. Welsh (1983*b*) has measured the kinetics of furosemide effects in epinephrine-stimulated intact dog trachea. They reported a 48% inhibition of I_{sc} with a half-time of ~5 min, in good agreement with model predictions. Cl secretion (J^{tc}_{Cl}) fell from 2.23 μeq · cm^{-2} · h^{-1} to 0.15 μeq · cm^{-2} · h^{-1}, whereas Na absorption increased slightly from 0.65 μeq · cm^{-2} · h^{-1} to 0.79 μeq · cm^{-2} · h^{-1}. Calculated final membrane potential (−69 mV) and apical (768 Ω · cm^2) and basolateral membrane (434 Ω · cm^2) resistances are also consistent with these experimental results. The fall in $[Cl]_c$ and the relatively small changes in $[Na]_c$ and $[K]_c$ predicted by the model are in good agreement with isotope and atomic absorption data of Widdicombe et al. (1983). Of note, the model effectively described transient phenomena even though only steady-state data were incorporated in the model formulation.

In contrast to results for transport inhibition by furosemide and ouabain, inhibition of ionic channels (Figs. 2, *C–E*) resulted in an immediate change in I_{sc}, tissue conductance, and membrane potential. For inhibition of the apical Cl conductance with DPC, the immediate hyperpolarization was followed by a slow depolarization because of a decrease in cell K activity. Inhibition of the apical Na channel by amiloride or the apical Cl channel by DPC resulted in immediate hyperpolarization as expected.

Cellular response to Cl-channel activation

Fig. 3 (*left*) shows the time course of membrane potential, resistance, cell ionic concentrations, and transport rates in response to sudden activation of the apical Cl conductance. The corresponding short-current response is given in Fig. 3 (*right, curve labeled 50 μm*). Where indicated, Cl conductance was increased 10-fold (see legend), as expected in various experimental maneuvers. Surprisingly, the response in I_{sc} was biphasic with an immediate increase in I_{sc} followed by a slower decrease to a level greater than the baseline I_{sc}. Examination of the time course of individual parameters provides an explanation for this observation. Activation of the Cl conductance

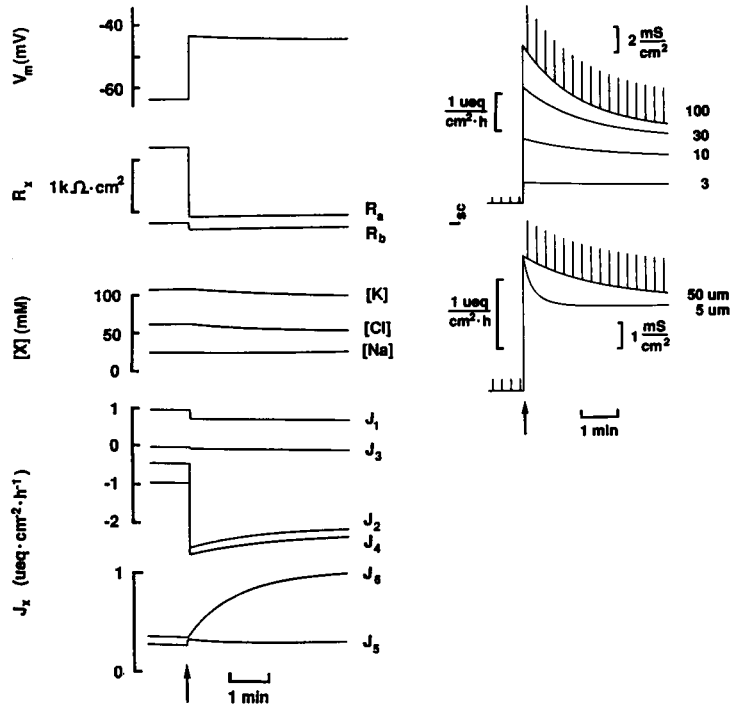

FIGURE 3 Time course of membrane potential, membrane resistance, intracellular ion concentrations, and short-circuit current in response to a sudden and persistent stimulation (at arrow) of the apical Cl conductance in intact trachea. P_3 was reduced for 10 min to 10% of the value given in Table 2 before stimulation indicated by the arrow. Before stimulation, I_{sc} was 1.37 μeq · cm^{-2} · h^{-1} with a membrane potential of −64 mV. (*Left*) Initial values before stimulation were: R_a = 1656 Ω · cm², R_b = 454 Ω · cm², J_5 = 0.40 μeq · cm^{-2} · h^{-1}, and J_6 = 0.23 μeq · cm^{-2} · h^{-1}. (*Right, top*) Influence of the magnitude of the increase in Cl conductance on I_{sc}. Cell height was 50 μm. P_3 was increased 3–100-fold (initial value 4.23 × 10^{-3} cm · h^{-1}) at the time marked by the arrow. (*Right, bottom*) Influence of cell volume on time course of I_{sc}. P_3 was increased from 4.23 × 10^{-3} cm · h^{-1} to 4.23 × 10^{-2} cm · h^{-1} at the arrow. Cell height was 50 and 5 μm, as indicated.

causes an immediate depolarization, leading to a large change in the transport rates of the apical Cl conductance (J_2) and the basolateral K conductance (J_4). The resultant decrease in cell Cl causes a time-dependent decrease in apical Cl flux, which is the main determinant of I_{sc}; there is a corresponding small increase in Na/K/2 Cl symport (J_6).

Fig. 3 (*right*) shows the relationship between the magnitude of stimulation of the apical Cl conductance and the time course of I_{sc}. With increasing Cl conductance, there is a saturable increase in maximal I_{sc}, and a more pronounced decline in I_{sc} after the rapid increase. The decrease in I_{sc} was faster with a smaller cell volume; of note, cell height in cultured tracheal cell monolayers (~5 μm) is much less than that of the intact trachea (50 μm). This difference is important when comparing kinetic data from cultured cells and intact trachea. It is interesting that the general shape of the I_{sc} curve has some characteristics similar to that measured in response to hormonal effectors of Cl conductance in intact and cultured trachea (Coleman et al., 1984; Leikauf et al., 1985; Tamaoki et al., 1988), despite continued elevation in the Cl conductance.

The role of K in Na/Cl symport

Secondary active cation-coupled Cl symport is essential for continuous Cl secretion, however, the responsible protein has not been identified or characterized in tracheal epithelium. Two electroneutral modes of this symporter have been proposed: Na/Cl and Na/K/2 Cl cotransport. Experimental results by Fong and Widdicombe (1989) and Welsh (1984) favor Na/K/2 Cl symport, whereas other reports obtained in dispersed isolated cells favor Na/Cl symport (Widdicombe et al., 1983; Musch and Field, 1989). The K dependence in each transporting unit may be under hormonal control, as suggested by recent experiments in the kidney thick ascending limb (Sun and Hebert, 1989).

Several possible experimental maneuvers were evaluated theoretically to distinguish between Na/K/2 Cl and Na/Cl symport mechanisms. The most discriminating experiments involved K-ion substitution and inhibition of basolateral K conductance. In response to 100% inhibition of the basolateral K conductance, model calculations show a 67% inhibition of I_{sc} if Cl enters the cell by Na/Cl symport and an 83% inhibition for Na/K/2 Cl symport.

In cultured dog tracheal epithelial cells, Fong and Widdicombe (1989) reported a maximal inhibition by barium of 83 ± 4% inhibition of I_{sc} in response to addition of 5 mM barium to the serosal solution, supporting Na/K/2 Cl symport.

Removal of external K is another effective procedure to discriminate between Na/Cl (Fig. 4 *A*) and Na/K/2 Cl (Fig. 4 *B*) symport. In both cases, removal of external K inhibited the 3 Na/2 K ATPase immediately. Because Na/Cl symport is not affected directly by $[K]_a$, this symporter continued to transport Na and Cl into the cell when favorable electrochemical gradients were present (>10 min in the calculation). As shown in Fig. 4 *A*, $[Na]_c$ increased and $[K]_c$ decreased, leading to a slow depolarization. Cell Na accumulated because of Na/Cl symport and apical Cl conductance; cell K was depleted because of conductive basolateral exit. $[Cl]_c$ increased slightly in response to the membrane depolarization. Net ion movement resulted in a 16% increase in cell volume over 10 min. The Na/K/2 Cl symporter (Fig. 4 *B*) reversed its direction upon K removal, leading to a rapid loss of ions, accompanied by cell shrinkage (35% within 10 min). Membrane potential hyperpolarized over this time, resulting in the loss of Cl via the cotransporter and the apical conductance. Therefore the K dependence of the basolateral symporter should strongly influence the time course of $[Cl]_c$ and membrane potential. In subsequent calculations it was assumed that basolateral symport is K dependent.

Simulation of intracellular transients in Cl

Ion substitution experiments are frequently performed to examine transport mechanisms in polarized epithelial

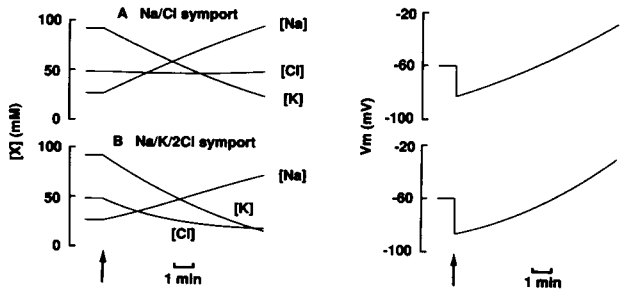

FIGURE 4 Response of cell ion activities and membrane potential to K removal from mucosal and serosal solutions assuming (*A*) Na/Cl or (*B*) Na/K/2 Cl symport under short-circuit conditions. Steady-state transcellular fluxes were appropriate for primary cultures of dog tracheal epithelia ($J^{tc}_{Na} = 0.19$ μeq · cm^{-2} · h^{-1}; $J^{tc}_{Cl} = -0.09$ μeq · cm^{-2} · h^{-1}). Cell volume was 5 μl · cm^{-2}. $[K]_a$ and $[K]_b$ were reduced from 4.05 to 0.04 mM.

cells. Two types of ion substitution studies have been performed in dog tracheal cells in primary culture. Both exhibit asymmetric behavior which requires quantitative modeling. Chao et al. (1990) measured I_{sc} in response to rapid Cl removal from and addition to solutions bathing the mucosal and serosal membranes. Cl removal resulted in a rapid increase in I_{sc}, followed by a slower decrease to a value below baseline. Cl addition results in a rapid decrease in I_{sc}, with magnitude smaller than the increase observed upon Cl removal.

The mathematical model predicts an asymmetrical time course of I_{sc} in the absence of furosemide (Fig. 5 *A*, *left*) in good agreement with experiment (Chao et al., 1990). The reason for the asymmetry is the increased contribution of the symporter to Cl entry compared with Cl exit, resulting in a decrease in the ionic Cl current which flows in the Cl addition experiment. This hypothesis was confirmed by showing that the magnitude of the I_{sc} response becomes symmetrical upon complete inhibition of the symporter (Fig. 5 *B*) in agreement with experimental data shown in Fig. 5 *C*.

To examine the mechanism for the slow change in I_{sc} after Cl addition and removal, cell Cl activity was measured recently using the Cl-sensitive fluorescent indicator SPQ (Chao et al., 1990). SPQ fluorescence (F) is related to $[Cl]_c$ by the Stern-Volmer relation:

$$F/F_o = (1 + K_q[Cl]_c)^{-1}, \quad (13)$$

where F_0 is fluorescence in the absence of Cl and K_q is the Stern-Volmer constant for quenching of SPQ by Cl (13 M^{-1} in tracheal cells). Cl transport mechanisms were examined from the time course of cell fluorescence in response to Cl addition to and removal from bathing solutions. The time course of $[Cl]_c$ predicted by the model (Fig. 5, *A* and *B*, *right*) is similar to the time course of the slower change in I_{sc}, and agrees well with the experimental data shown in Fig. 5 *C*, right.

Regulation of secretion by Ca and cAMP agonists

Cytoplasmic Ca and cAMP have been shown to be important intracellular signals for the action of secretagogues in epithelial cells. In tracheal epithelia, both the apical Cl conductance and the basolateral K conductance are possible target sites for regulation of secretion by Ca and cAMP-dependent pathways (Welsh, 1985). Experimentally, the Ca pathway has been stimulated by bradykinin in the presence of indomethacin (to prevent prostaglandin-induced cAMP production), and the cAMP pathway by cell permeable analogues of cAMP (Leikauf et al., 1985; McCann et al., 1989). It has been proposed that some secretagogues including isoproterenol act through both pathways, giving composite responses in

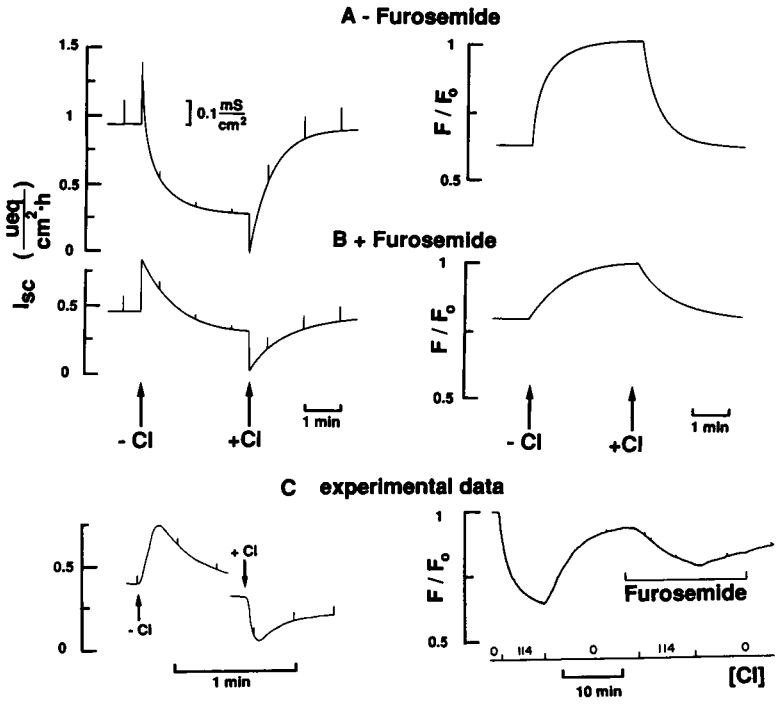

FIGURE 5 Effects of changes in external [Cl] on short-circuit current (*left*) and intracellular Cl activity (*right*) in secreting primary tracheal epithelium. (*A*, *B*) Simulated data. $[Cl]_a$ and $[Cl]_b$ were changed from 93 to 1 to 93 mM in the absence (*A*) or presence (*B*) of furosemide (to inhibit Na/K/2 Cl symport by 90%). Model parameters: $J^{tc}_{Na} = 0.19\ \mu eq \cdot cm^{-2} \cdot h^{-1}$, $J^{tc}_{Cl} = -0.70\ \mu eq \cdot cm^{-2} \cdot h^{-1}$, and membrane potential = −40 mV. (*Right*) Time course of intracellular SPQ fluorescence (related to $[Cl]_c$ by Eq. 13) in response to Cl addition (93 mM) and removal (1 mM) from mucosal and serosal solution. Parameters: $P_1 = 9.49 \times 10^{-4}$ cm · h^{-1}, $P_2 = 6.71 \times 10^{-4}$ cm · h^{-1}, $P_3 = 2.09 \times 10^{-2}$ cm · h^{-1}, $P_4 = 3.29 \times 10^{-2}$ cm · h^{-1}, $P_5 = 1.24\ \mu mol \cdot cm^{-2} \cdot h^{-1}$, $P_7 = 1.93 \times 10^{-4}$ cm · h^{-1} · mM^{-1}. (*C*) Experimental data taken from Chao et al. (1990) showing effects of removal and addition of 114 mM Cl to solutions bathing the mucosal and serosal surfaces of a dog tracheal monolayer. The I_{sc} experiment (*left*) was performed in the presence of furosemide; the spikes are in the measured units of $\mu eq \cdot cm^{-2} \cdot h^{-1}$.

short-circuit experiments (Smith et al., 1989). A typical experimental curve is given at the bottom of Fig. 6. To examine possible mechanisms for the tissue response to secretagogues, time-dependent effects of Ca, cAMP, and Ca + cAMP stimulation on Cl and K conductances were modeled.

Fig. 6 *A* shows the stimulation of I_{sc} assuming that Ca acts on the apical Cl conductance. I_{sc} and tissue conductance increase rapidly; I_{sc} decreases slightly below baseline levels and reaches baseline level a few minutes after stimulation. As shown above, persistent activation of the Cl conductance would lead to a significant elevation in steady-state I_{sc}. There is a depolarization from −67 to −32 mV at the time of increased I_{sc}, followed by repolarization to the initial value.

Fig. 6 *B* shows activation of the Cl conductance by cAMP. There is a slow increase in I_{sc} to a stable elevated value as observed experimentally. Because of the slow onset of the cAMP effect, the overshoot phenomenon as shown in Fig. 3 was not observed. Figs. 6, *C* and *D* show the composite I_{sc} response when both Ca and cAMP-dependent pathways are activated. In Fig. 6 *C*, the apical Cl conductance is the target site for activation, whereas in Fig. 6 *D*, the basolateral K conductance is activated. There was a biphasic response with a steady-state I_{sc} greater than the baseline value, similar to results reported for the agonist isoproterenol or bradykinin in the absence of indomethacin (Smith et al., 1989; Hartmann et al., 1989). Ca and cAMP-dependent stimulation of the K conductance (Fig. 6 *D*) leads to a transient increase in I_{sc}, however, the magnitude of this increase is much less than that observed for stimulation of the Cl conductance. This difference in maximal stimulation of I_{sc} is more pronounced in the presence of amiloride (inhibition of apical Na conductance) or in tissue with low transcellular Cl secretion ($J_2 = -0.2\ \mu eq \cdot cm^{-2} \cdot h^{-1}$; not shown). Comparison of the calculated results with experiment (Welsh, 1986) suggests that the action of Ca-dependent agonists cannot be directed to the K conductance only. In addition, activation of a K conductance results in a transient hyperpolarization from −67 to −76 mV, opposite to the predicted effect of activation of Cl conductance.

Inhibition of the basolateral K conductance by 50% (Fig. 6 *E*) and 90% (Fig. 6 *F*) leads to marked decrease

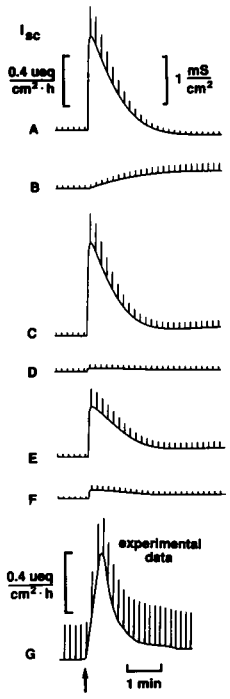

FIGURE 6 Time course of short-circuit current in response to stimulation of apical Cl conductance or basolateral K conductance by Ca and cAMP. In simulated data (*A–F*) permeability coefficients are identical to those in Fig 4. Apical Na conductance was inhibited by 70% at 5 min before and during stimulation (to allow a new steady state to be achieved). (*A*) Stimulation of Cl conductance by Ca as described by Eqs. 10 and 11 with $P_* = P_3$ ($A = 0.175\ nm^{-1}$, $B = 16.5$). (*B*) cAMP stimulation of Cl conductance as described by Eq. 12 with $C = 10$ and $P_* = P_3$. (*C*) Simultaneous stimulation of Cl conductance by Ca and cAMP-dependent pathways. Parameters A, B, and C (see Eqs. 10–12) as described above. (*D*) Stimulation of the basolateral K-conductance by Ca and cAMP. Same parameters A, B, and C for Eqs. 10–12 were used as in Fig. 6 *C*. (*E–F*) Effect of inhibition of basolateral K conductance on Ca-dependent stimulation of short-circuit current. P_4 was decreased by 50% (Fig. 6 *E*) and 90% (Fig. 6 *F*) 5 min before stimulation of the Cl conductance by Ca and cAMP. (*G*) Experimental data showing I_{sc} in response to 10 μM isoproterenol added to the serosal solution at the arrow (Hartmann et al., 1989). The spikes (units μeq · cm^{-2} · h^{-1}) represent parallel transcellular and paracellular conductances.

in Cl secretion (see Fig. 6 *A* for comparison). Experimentally, K conductance has been reduced using $BaCl_2$. In the presence of $BaCl_2$, epinephrine did not stimulate Cl flux as measured by short-circuit current (Welsh, 1983*d*).

DISCUSSION

A quantitative kinetic model was developed to predict steady-state and non-steady-state phenomena in secretory epithelial cells, in which Cl is transported through the cell via cation-coupled symport and contralateral conductance. The formulation of the model is general so that tracheal, intestinal, and sweat-duct secretory cells, and renal thick ascending limb and other epithelia can be modeled by selection of an appropriate set of initial parameters. The model can be evaluated under both open-circuit and short-circuit conditions so that electrical, chemical, and fluorescence measurements can be modeled for any magnitude of paracellular conductance. The calculations reported here were focused on the mechanism and regulation of salt secretion by tracheal epithelium. Parameters and experimental results were selected from the canine trachea because an extensive data set is available on electrochemical parameters, transepithelial ion fluxes, and intracellular signaling mechanisms. The purpose of the model was to examine the way in which individual membrane transporters interact under baseline conditions and when stimulated by secretagogues, and to interpret data related to controversial issues. In addition, the model aided in the design of studies to test opposing hypotheses, for example, the measurement of intracellular Cl activity and membrane potential to discriminate between Na/K/2 Cl and Na/Cl symport. The model should be of use in incorporating future experimental findings into the secretory mechanism.

The mathematical formulation of the model was kinetic, rather than purely thermodynamic. The specific advantages of a kinetic model, as discussed by Latta et al. (1984) and Verkman and Alpern (1987), are that transporter saturabilities, allosteric dependences, and coupling stoichiometries can be specified explicitly. This formulation was particularly important in the trachea because of the complexity of the transporters and the need to simulate transport inhibition and ion substitution experiments which cause large perturbations from the steady state.

The apical and basolateral membrane Na, K, and Cl transporters selected for the model formulation were based on the consensus of findings in a substantial number of transport and patch-clamp studies on intact and cultured tracheal epithelia. The apical Cl conductance and basolateral K conductance, symporter, and 3 Na/2 K ATPase are of central importance to the secretory mechanism. Because of conflicting data regarding the K dependence of the basolateral symporter and because of the possibility of hormonal regulation, both Na/K/2 Cl and Na/Cl symport were evaluated. The presence of an amiloride-inhibitable apical Na conductance has been clearly demonstrated (Widdicombe and Welsh, 1980; Cullen and Welsh, 1987; Welsh et al., 1983). Although the apical Na conductance had minimal influence on the calculated results, its inclusion was justified and potentially important in modeling ion substitution experiments. A small apical K conductance was included in the model

as suggested in a number of studies (Boucher et al., 1981; Welsh, 1983*a*). The apical K conductance was important in a recent electrical model of net Cl secretion in trachea by Cook and Young (1989). In contrast to the model of Cook and Young, our model included the characteristics of individual membrane transporters and was formulated specifically to examine the kinetics of membrane potential and intracellular ion activities in response to selected modification of membrane transporter activities.

There were several assumptions made in the model which we believe are justified, or at least necessary, given the current state of knowledge. The specific form of the flux equations for the tracheal 3 Na/2 K ATPase and the cation-coupled Cl symporter were chosen based on incomplete knowledge about ion saturabilities and detailed transport mechanism. The results of the model should be insensitive to the precise form of these flux equations, particularly for semi-quantitative comparisons of experiment with theory. It was assumed that the cell was in instantaneous osmotic equilibrium and that cell volume regulation was absent. This assumption is justified for the simulations presented because of the small cell volume changes and the slow change in cell ionic content. Of note, this model will be of use in examining possible mechanisms of cell volume regulation when data become available. The model contained only Na, K, and Cl as intracellular ions, and an unspecified impermeant molecule(s). Changes in pH and HCO_3 that might be mediated by Na/H or Cl/HCO_3 antiporters were neglected because these transporting systems have not been demonstrated and little is known about the nature of pH-regulatory processes in the trachea. We would expect little influence of neglecting pH effects because HCO_3 is nominally absent in most of the measurements that were simulated, and because the trachea is known to transport NaCl but not $NaHCO_3$. In addition, agonist-induced activation of the Na/H antiporter in a number of cell types causes small pH changes (<0.3 pH units) and generally occurs on a slower time scale than Ca elevations (Moolenaar, 1986); in HCO_3-free media, these changes are greatly diminished (Bierman et al., 1988; Ganz et al., 1989). Finally, the model does not contain organic molecules such as glucose and amino acids, which are likely to be of minimal influence on the results presented.

A novel aspect of this model was the inclusion of transport regulation by intracellular second messengers. Assuming a linear coupling relationship between intracellular ionized Ca and the activation of apical Cl conductance, the calculated time course of I_{sc} was in good agreement with experiments. It was shown that the basolateral membrane K conductance could not be the sole target site for regulation of secretion by Ca-dependent agonists. In addition, it was possible to simulate the action of cAMP analogues and isoproterenol, an agonist thought to act on both Ca and cAMP-dependent transport pathways. It must be recognized that the calculations involving regulation require inclusion of additional assumptions which cannot be justified rigorously. As new information on the concentration and time dependences of second messenger generation and/or its effects on individual transport systems become available, models of transport regulation should have an improved predictive value on the kinetic analysis of experiments in intact tissue, where several transporters interact.

We thank J. H. Widdicombe and M. Kondo for interpretation of experimental results and helpful discussions on simulations.

This work was supported by National Institutes of Health grants DK39354, HL42368, and DK35124, a grant from the Cystic Fibrosis Foundation and a grant-in-aid from the American Heart Association. T. Hartmann was supported by a post-doctoral fellowship of the Deutsche Forschungsgemeinschaft. A. S. Verkman is an established investigator of the American Heart Association.

Received for publication 2 January 1990 and in final form 9 April 1990.

REFERENCES

Apell, H. J. 1989. Electrogenic properties of the Na, K pump. *J. Membr. Biol.* 110:103–114.

Bierman, A. J., E. J. Cragoe Jr., S. W. de Laat, and W. H. Moolenaar. 1988. Bicarbonate determines cytoplasmic pH and suppresses mitogen-induced alkalinization in fibroblastic cells. *J. Biol. Chem.* 263:15253–15256.

Boucher, R. C., M. J. Stutts, and J. T. Gatzy. 1981. Regional differences in bioelectric properties and ion flow in excised canine airways. *J. Appl. Physiol.* 51:706–714.

Chao, A. C., J. H. Widdicombe, and A. S. Verkman. 1990. Chloride conductive and cotransport mechanisms in cultures of tracheal epithelial cells measured by an entrapped fluorescent indicator. *J. Membr. Biol.* 113:193–202.

Coleman, D., I. Tuet, and J. H. Widdicombe. 1984. Electrical properties of dog tracheal epithelial cells grown in monolayer culture. *Am. J. Physiol.* 246:C355–C359.

Cook, D. I., and J. A. Young. 1989. Effect of K+ channels in the apical plasma membrane on epithelial secretion based on secondary active Cl^- transport. *J. Membr. Biol.* 110:139–146.

Cullen, J. J., and M. J. Welsh. 1987. Regulation of sodium absorption by canine tracheal epithelium. *J. Clin. Invest.* 79:73–79.

Finkbeiner, W., and J. Widdicombe. 1990. Control of nasal airway secretion, ion transport, and water movement. *In* Defence capabilities of the respiratory tract. R. Schlesinger, editor. Raven Press, New York. In press.

Fong, P., and J. H. Widdicombe. 1989. Potassium dependence of the basolateral chloride uptake mechanism in primary cultures of canine tracheal epithelium. *Biophys. J.* 55:606*a*. (Abstr.)

Ganz, M. B., G. Boyarsky, R. B. Sterzel, and W. F. Boron. 1989. Arginine vasopressin enhances pHi regulation in the presence of $HCO3^-$ by stimulating three acid-base transport systems. *Nature (Lond.).* 337:648–651.

Goldschlegger, R., S. J. D. Karlish, A. Rephaeli, and W. D. Stein. 1987. The effect of membrane potential on the mammalian sodium-potassium pump reconstituted into phospholipid vesicles. *J. Physiol.* 387:331–355.

Hartmann, T., M. Kondo, A. S. Verkman, and J. H. Widdicombe. 1989. Calcium dependent stimulation of chloride secretion in cultured dog tracheal epithelial cells. *J. Cell Biol.* 109:303*a*. (Abstr.)

Latta, R., C. Clausen, and L. C. Moore. 1984. General method for the derivation and numerical solution of epithelial transport models. *J. Membr. Biol.* 82:67–82.

Lederer, W. J., and M. T. Nelson. 1984. Sodium pump stoichiometry determined by simultaneous measurements of sodium efflux and membrane current in barnacle. *J. Physiol.* 348:665–677.

Leikauf G., I. Ueki, J. Nadel, and J. H. Widdicombe. 1985. Bradykinin stimulates chloride secretion and prostaglandin E2 release by canine tracheal epithelium. *Am. J. Physiol.* 248:F48–F55.

McCann J. D., R. C. Bhalla, and M. Welsh. 1989. Release of intracellular calcium by two different second messengers in airway epithelium. *Am. J. Physiol.* 257:L116–L124.

McRoberts, J. A., S. Erlinger, M. J. Rindler, and M. H. Saier, Jr. 1982. Furosemide-sensitive salt transport in the Madin-Darby canine kidney cell line. *J. Biol. Chem.* 257:2260–2266.

Milanick, M. A., and J. F. Hoffman. 1986. Ouabain sensitive Na/K exchange, Na/Na exchange and uncoupled Na efflux are insensitive to changes in membrane potential, Em, in intact human red blood cells. *Biophys. J.* 49:548*a*. (Abstr.)

Moolenaar, W. H. 1986. Effects of growth factors on intracellular pH regulation. *Annu. Rev. Physiol.* 48:363–376.

Musch, M. W., and M. Field. 1989. K-independent Na-Cl cotransport in bovine tracheal epithelial cells. *Am. J. Physiol.* 256:C658–C665.

O'Grady, S. M., M. W. Musch, and M. Field. 1986. Stoichiometry and ion affinities of the Na-K-Cl-cotransport system in the intestine of the winter flounder (Pseudopleuronectes americanus). *J. Membr. Biol.* 91:33–41.

Owen, N., and M. L. Prastein. 1985. Na/K/Cl cotransport in cultured human fibroblasts. *J. Biol. Chem.* 260:1445–1451.

Rakowski, R. F., D. C. Gadsby, and P. Deweer. 1989. Stoichiometry and voltage dependence of the sodium pump in voltage-clamped, internally dialyzed squid giant axon. *J. Gen. Physiol.* 93:903–941.

Shorofsky, S. R., M. Field, and H. A. Fozzard. 1984. Mechanism of Cl secretion in canine trachea: changes in intracellular chloride activity with secretion. *J. Membr. Biol.* 81:1–8.

Shorofsky, S. R., M. Field, and H. A. Fozzard. 1986. Changes in intracellular sodium with chloride secretion in dog tracheal epithelium. *Am. J. Physiol.* 250:C646–C650.

Smith, J. J., J. D. McCann, and M. J. Welsh. 1989. Bradykinin-induced chloride secretion in canine tracheal epithelium is coupled to two separate secondary messengers. *Am. Rev. Respir. Dis.* 139:A477.

Smith, P. L., and R. A. Frizzell. 1984. Chloride secretion by canine tracheal epithelium. *J. Membr. Biol.* 77:187–199.

Sun, A. M., and S. C. Hebert. 1989. ADH alters the K^+ requirement for the luminal furosemide-sensitive NaCl symporter in mouse medullary thick limbs. *Kidney Int.* 35:489.

Tamaoki J., I. Ueki, J. H. Widdicombe, and J. Nadel. 1988. Stimulation of Cl secretion by neurokinin A and neurokinin B in canine tracheal epithelium. *Am. Rev. Respir. Dis.* 137:899–902.

Verkman A. S., and R. J. Alpern. 1987. Kinetic transport model for cellular regulation of pH and solute concentration in the renal proximal tubule. *Biophys. J.* 51:533–546.

Welsh, M. J. 1983*a*. Evidence for basolateral membrane potassium conductance in canine tracheal epithelium. *Am. J. Physiol.* 244:C377–C384.

Welsh, M. J. 1983*b*. Inhibition of chloride secretion by furosemide in canine tracheal epithelium. *J. Membr. Biol.* 71:219–236.

Welsh, M. J. 1983*c*. Intracellular chloride activities in canine tracheal epithelium. *J. Clin. Invest.* 71:1392–1401.

Welsh, M. J. 1983*d*. Barium inhibition of basolateral membrane potassium conductance in tracheal epithelium. *Am. J. Physiol.* 244:F639–F645.

Welsh, M. J. 1984. Energetics of chloride secretion in canine tracheal epithelium: comparison of the metabolic cost of chloride transport with the metabolic cost of sodium transport. *J. Clin. Invest.* 74:262–268.

Welsh, M. J. 1985. Intracellular calcium regulates basolateral potassium channels in a chloride secreting tissue. *Proc. Natl. Acad. Sci. USA.* 82:8823–8826.

Welsh, M. J. 1986. Adrenergic regulation of ion transport by primary cultures of canine tracheal epithelium: cellular electrophysiology. *J. Membr. Biol.* 91:121–128.

Welsh, M. J. 1987. Electrolyte transport by airway epithelium. *Physiol. Rev.* 67:1143–1184.

Welsh, M. J., P. L. Smith, and R. A. Frizzell. 1983. Chloride secretion by canine tracheal epithelium: III. Membrane resistances and electromotive forces. *J. Membr. Biol.* 71:209–218.

Westenfelder, C., W. R. Earnest, and F. J. Al-Bazzaz. 1980. Characterization of Na-K-ATPase in dog tracheal epithelium: enzymatic and ion transport measurements. *J. Appl. Physiol.* 48(6):1008–1019.

Widdicombe, J. H., and M. J. Welsh. 1980. Ion transport by dog tracheal epithelium. *Fed. Proc.* 39:3062–3066.

Widdicombe, J. H., I. F. Veki, I. Bruderman, and J. A. Nadel. 1979. The effects of sodium substitution and oubain on ion transport by dog tracheal epithelium. *Am. Rev. Respir. Dis.* 120:385.

Widdicombe, J. H., C. B. Basbaum, and E. Highland. 1981. Ion contents and other properties of isolated cells from the dog tracheal epithelium. *Am. J. Physiol.* 241:C184–C192.

Widdicombe, J. H., I. T. Nathanson, and E. Highland. 1983. Effects of loop diuretics on ion transport by dog tracheal epithelium. *Am. J. Physiol.* 245:C388–C396.

Widdicombe, J. H., D. L. Coleman, W. E. Finkbeiner, and D. S. Friend. 1987. Primary cultures of the dog's tracheal epithelium: fine structure, fluid, and electrolyte transport. *Cell Tissue Res.* 247:95–103.